## PCCP



## **PAPER**



Cite this: Phys. Chem. Chem. Phys., 2020, 22, 25011

Received 2nd September 2020 Accepted 19th October 2020

DOI: 10.1039/d0cp04634e

rsc.li/pccp

# Adsorption properties of acrolein, propanal, 2-propenol, and 1-propanol on Ag(111)

Mark Muir, David L. Molina, Arephin Islam, D. Mohammed K. Abdel-Rahman and Michael Trenary \*\*

Reflection absorption infrared spectroscopy and temperature programmed desorption were used to study the adsorption of acrolein, its partial hydrogenation products, propanal and 2-propenol, and its full hydrogenation product, 1-propanol on the Aq(111) surface. Each molecule adsorbs weakly to the surface and desorbs without reaction at temperatures below 220 K. For acrolein, the out-of plane bending modes are more intense than the C=O stretch at all coverages, indicating that the molecular plane is mainly parallel to the surface. The two alcohols, 2-propenol and 1-propanol, have notably higher desorption temperatures than acrolein and display strong hydrogen bonding in the multilayers as revealed by a broadened and redshifted O-H stretch. For 1-propanol, annealing the surface to 180 K disrupts the hydrogen-bonding to produce unusally narrow peaks, including one at 1015 cm<sup>-1</sup> with a full width at half maximum of 1.1 cm<sup>-1</sup>. This suggests that 1-propanol forms a highly orderded monolayer and adsorbs as a single conformer. For 2-propenol, hydrogen bonding in the multilayer correlates with observation of the C=C stretch at 1646 cm<sup>-1</sup>, which is invisible for the monolayer. This suggests that for monolayer coverages. 2-propenol bonds with the C=C bond parallel to the surface. Similarly, the C=O stretch of propanal is very weak for low coverages but becomes the largest peak for the multilayer, indicating a change in orientation with coverage.

## 1. Introduction

The selective hydrogenation of  $\alpha,\beta$ -unsaturated aldehydes is an important process for numerous industrial applications as the allylic alcohols are valuable intermediates in the production of pharmaceuticals, perfumes, and flavorings. 1-4 The simplest α,β-unsaturated aldehyde, acrolein (C<sub>3</sub>H<sub>4</sub>O), is difficult to hydrogenate to 2-propenol (allyl alcohol) because there are no substituents on the C=C group to destabilize the interaction with the catalyst surface. 5-7 Generally, it has been established that thermodynamics favours hydrogenation at the C=C bond to form the saturated aldehyde. Therefore, a kinetic manipulation is required to hydrogenate at the C=O bond to form the desired product, the unsaturated alcohol.<sup>7</sup>

Aside from the reactivity of the metal catalyst, the orientation of the adsorbate on the surface must be considered. Tuokko et al. found using density functional theory (DFT) calculations that the selective hydrogenation of acrolein on Pd(111) and Pt(111) are governed by steric effects of the adsorbate. They show that with increasing acrolein coverage, the selectivity decreases.<sup>8</sup> Brandt et al. showed using near edge x-ray absorption fine structure (NEXAFS) that acrolein on Ag(111) tilts at the C $\equiv$ C bond from 6°

Department of Chemistry, University of Illinois at Chicago, 845 W. Taylor St., Chicago, Illinois 60607, USA. E-mail: mtrenary@uic.edu

at 0.45 monolayer (ML) to  $12^{\circ}$  at 0.85 ML and that this tilt has an effect on the hydrogenation mechanism.9

Reflection absorption infrared spectroscopy is a powerful technique for determining the structural properties of reactants and products on well-defined single crystals. According to the surface infrared selection rule, a vibration will be RAIRS active if there is a non-zero projection of the dynamic dipole moment along the surface normal. In terms of group theory, the vibrational state can be accessed by an electric dipole transition from the ground vibrational state if the upper state belongs to the same irreducible representation as the surface normal. 10 Therefore, infrared spectroscopy can give valuable insight into the adsorption geometry on metal surfaces at a wide range of coverages and pressures.

The selectivity in acrolein hydrogenation depends not only on the structure and stability of adsorbed acrolein, but also on the way the three hydrogenation products bond to the surface. These four molecules interact weakly with Ag(111), and in the absence of coadsorbed hydrogen, desorb without reaction. The weakness of the interaction with the surface implies that they adsorb primarily through  $\pi$ -bonding involving the C=O or C=C groups, or through dative bonding involving the oxygen lone pairs of the OH groups. The weak bonding to the surface implies that prior vibrational studies of the molecules in the gas, liquid, or solid phases, or dissolved in inert solvents or

trapped in inert gas matrices, will be applicable to the RAIR spectra of these molecules on Ag(111).

An important factor in the vibrational spectra of these molecules is the existence of various rotational conformers. The different conformers have relative stabilities that are generally known from either experiment or theory and are typically separated in energy by a few hundred cm<sup>-1</sup> (a few kJ mol<sup>-1</sup>). However, interaction with the surface may significantly alter the relative conformer stability. The planar acrolein molecule can exist in two forms, *cis* and *trans*, depending on the relative orientation of the C=O and C=C bonds. Spectroscopic measurements have shown that *trans* acrolein is most stable.<sup>11</sup>

Propanal has two stable conformers in the gas phase, *cis* and *gauche*, with the *cis* form more stable. The energy difference of the two forms has been reported as:  $420 \pm 27 \text{ cm}^{-1}$  by Randell *et al.* in a microwave and far-IR study;  $^{12}$  315  $\pm$  35 cm $^{-1}$  by Pickett and Scroggin $^{13}$  in a microwave study; and  $370 \pm 21 \text{ cm}^{-1}$  in an IR study by Guirgis *et al.* of propanal dissolved in liquid Xe. Theoretical calculations indicated that the *cis* conformer is more stable by  $309 \text{ cm}^{-1}$ . With the carbon atoms labelled as  $H_3C(3)C(2)-H_2C(1)HO$ , then in the *cis* form the three C atoms and the O atom lie in a plane, while in the *gauche* form, the  $H_3C(3)$  group is at a dihedral angle of  $128.2^{\circ}$  with respect to the C(2)C(1)HO plane.  $^{14}$ 

There are five possible stable conformers for 2-propenol. <sup>15</sup> These conformers arise because the OH group can be either *cis* or *gauche* (C or G) to the C=C double bond, and the angular position of the OH group around the CO bond can be either *trans* (t), *gauche* (g), or *gauche'* (g'). The Gg conformer was found to be lowest in energy, with the Cg, Ct, and Gt conformers higher by  $135 \pm 14$ ,  $260 \pm 46$ ,  $337 \pm 75$  cm<sup>-1</sup>, respectively. No experimental evidence was found for the fifth conformer, but it was predicted theoretically to be 500 cm<sup>-1</sup> higher in energy than the Gg conformer. <sup>15</sup>

Five conformers of 1-propanol have been identified with closely spaced energies. <sup>16</sup> Similar to 2-propenol, these conformers arise because the OH group can be either *cis* or *gauche* (C or G) to the CH<sub>3</sub> group, and the angular position of the OH group around the CO bond can be either *trans* (t) or *gauche* (g). IR spectra have been measured for the liquid and for 1-propanol trapped in argon matrices and dissolved in CCl<sub>4</sub>. <sup>17</sup>

Although a comparative study of all four molecules adsorbed on Ag(111) has not been previously published, there are several relevant prior studies. Acrolein has been studied using vibrational spectroscopy on various surfaces, such as Au(111) and Ag(111),<sup>18</sup> a Ag thin film,<sup>19</sup> Pt(111),<sup>20</sup> Pd(111),<sup>21</sup> Ru(001),<sup>22</sup> and Ni/Pt(111).<sup>20</sup> By analysing the intensity of the out-of-plane modes (the =CH<sub>2</sub> wag, and the formyl and vinyl CH bends (CH<sub>f</sub>, and CH<sub>v</sub>)) relative to the intensity of the C=O stretch, the adsorption geometry can be inferred. On less reactive metals, such as Ag(111) and Au(111), the out-of-plane modes are much more intense than the C=O stretch, implying a parallel adsorption geometry. On the more reactive metals, the opposite is observed, indicating tilting at the C=O groups, with the tilt increasing with increasing coverage.

In studies similar to the present one, low-temperature RAIR spectra have been obtained for acrolein, 2-propenol, and propanal on Pd(111)<sup>21</sup> and for 2-propenol, propanal, and

1-propanol on Ru(001).<sup>23</sup> Adsorbed 1-propanol has been studied on Cu(111)<sup>24</sup> and 1-propanol and propanal have been studied on Rh(111),<sup>25</sup> Ni(111), Fe/Ni(111) and Cu/Ni(111).<sup>26</sup> Murillo *et al.* used high resolution electron energy loss spectroscopy to study acrolein, 2-propenol and propanal on a Pt–Ni–Pt(111) surface.<sup>20</sup> The desorption of propanal formed from the oxidation of propylamine on an oxygen-covered Au(111) surface has also been reported.<sup>27</sup>

## 2. Experimental details

The experiments were performed in an ultrahigh vacuum (UHV) chamber with a base pressure of  $1\times 10^{-10}$  Torr. The chamber is equipped with a PHI 10-155 cylindrical mirror analyzer for Auger electron spectroscopy (AES), PHI 15-120 optics for low energy electron diffraction (LEED), and a Hiden HAL201/3F quadrupole mass spectrometer for temperature programmed desorption (TPD). The UHV chamber is coupled to a Bruker IFS-66v/s Fourier-transform infrared (FTIR) spectrometer. The incident and reflected IR beams enter and exit the UHV chamber through differentially pumped, O-ring sealed KBr windows. A narrow band HgCdTe detector was used for most spectra, whereas an InSb detector was used for the C–H stretch region of adsorbed acrolein. The RAIR spectra were obtained at 4 cm $^{-1}$  resolution with 1024 scans and a linear heating rate of 1 K s $^{-1}$  was used for the TPD results.

The mounting of the Ag(111) crystal has been described elsewhere. The Ag(111) crystal was cleaned with Ar sputtering (1 keV, 8  $\mu$ A) and annealing to 800 K. The cleanliness of the surface was determined using LEED, AES, and RAIRS of adsorbed CO. Acrolein (96%, stabilized with hydroquinone, Alfa Aesar) was purified by successive freeze–pump–thaw cycles of liquid nitrogen followed by methanol/liquid nitrogen to eliminate possible decomposition products such as ethylene. 2-Propenol ( $\geq$ 99%, Sigma Aldrich Chemistry), propanal ( $\geq$ 99%, Acros Organics), and 1-propanol ( $\geq$ 99.5%, Sigma Aldrich) were purified with successive freeze–pump–thaw cycles of liquid nitrogen.

## 3. Results

The adsorption of each molecule on the Ag(111) surface was studied as a function of coverage with RAIRS and TPD. The coverages were based on TPD peak areas and the clear resolution between TPD peaks for monolayer and for higher layers. Therefore, one monolayer defined in this way corresponds to the saturation coverage of the first layer and will be somewhat less than one adsorbate molecule per surface Ag atom. For the RAIRS annealing experiments, the surface was dosed at 85 K, annealed to a given temperature and held there for one minute, then cooled back to 85 K where the spectra were acquired.

### 3.1 Acrolein

Fig. 1 shows the RAIR spectra of acrolein adsorbed on Ag(111) with increasing coverage at 85 K. At 0.17 and 0.29 ML, IR bands at 978, 991, 1007, and 1676 cm $^{-1}$  are observed. These bands correspond to the CH<sub>2</sub> out-of-plane wag (both the 978 and

**PCCP Paper** 

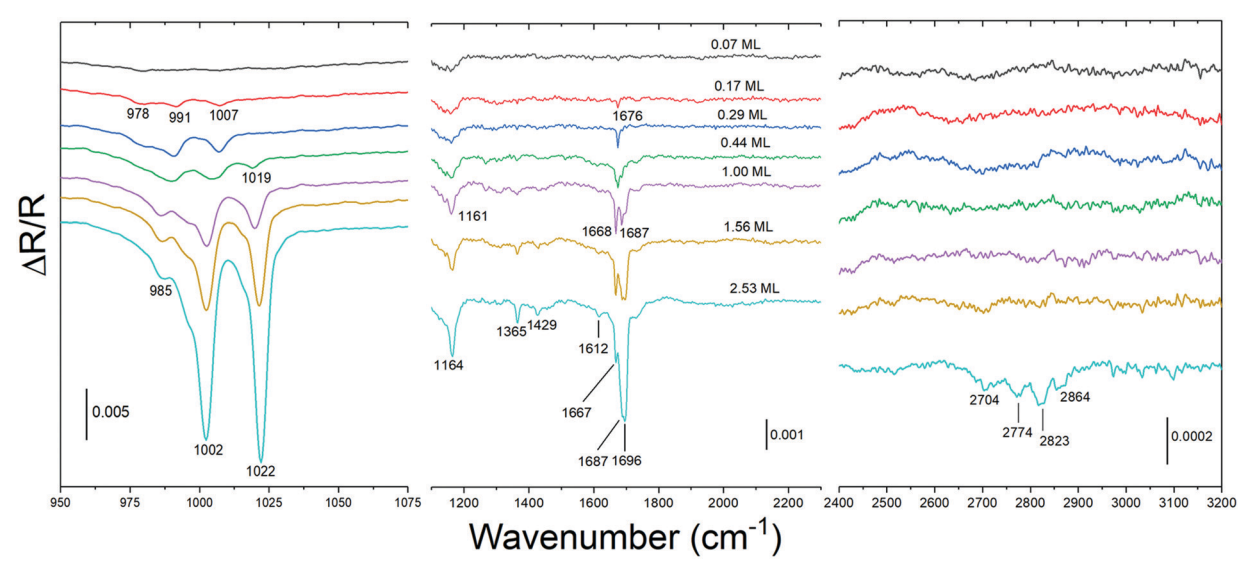


Fig. 1 RAIR spectra of acrolein adsorbed on Aq(111) at 85 K with increasing coverage.

991 cm<sup>-1</sup> peaks), the formyl CH out-of-plane bend, and the C=O stretch, respectively. In addition, for low coverages the C=O stretch is observed at 1676 cm<sup>-1</sup>, which is appreciably lower than the gas phase value of 1724 cm<sup>-1</sup>. Increasing the coverage redshifts the C=O stretch and gives rise to a secondary peak at 1687 cm<sup>-1</sup> beginning at 0.44 ML. This secondary peak is attributed to an interaction of the C=O bond with neighbouring acrolein molecules. With increasing coverage, the IR peak at 1007 cm<sup>-1</sup> redshifts and increases in intensity while a new IR peak at 1019 cm<sup>-1</sup> is observed. These two out-ofplane bending modes correspond to the CH groups (formyl and vinyl) and increase in intensity while the CH<sub>2</sub> wag (991 cm<sup>-1</sup>) remains relatively unchanged. The greater intensity of the outof-plane CH and CH2 wags over the C=O stretch implies a parallel bonding geometry, as noted by Itoh and co-workers for acrolein on Au(111) and Ag surfaces. 18,19

As multilayer acrolein forms on the Ag(111) surface, the IR peak at 1668 cm<sup>-1</sup> is further redshifted and the 1687 cm<sup>-1</sup> peak increases in intensity with a feature at 1696 cm<sup>-1</sup>. Of these three peaks, the C=O stretch at 1668 cm<sup>-1</sup> remains unchanged in intensity, indicating it is associated with the acrolein monolayer, while the second peak corresponds to a distortion due to neighbouring acrolein molecules. Additionally, the C-C stretching mode at 1161 cm<sup>-1</sup> becomes sharper and more intense above 1.00 ML. The formyl CH and the CH2 bending modes are observed in the multilayer at 1365 and 1429 cm<sup>-1</sup>, respectively. The C-H stretch region shows four features that are observed only at 2.53 ML. The peaks at 2704 and 2774 cm<sup>-1</sup> correspond to the formyl CH stretch and the first overtone of the vinyl CH bend, while the peaks at 2823 and 2864 cm<sup>-1</sup> corresponds to the CH<sub>2</sub> symmetric and antisymmetric stretches, respectively.

Puzzarini et al. compared calculated vibrational frequencies for trans and cis-acrolein to previous experimental gas phase and Ar matrix IR spectra. 11 A key difference in the trans and cis geometries of acrolein is the C-C stretch. In the gas phase, this vibration is at 1158 cm<sup>-1</sup> for trans-acrolein and at 1056 cm<sup>-1</sup>

Table 1 Comparison of vibrational assignments for acrolein multilayers on the surfaces of Au, Ag and Pd. The f and v subscripts refer to formyl and vinyl, respectively

| Mode                      | <i>Trans</i> -acrolein gas phase <sup>11</sup> | Ag(111)    | Ag film <sup>19</sup> | Au(111) <sup>18</sup> | Pd(111) <sup>21</sup> |
|---------------------------|--|------------|-----------------------|-----------------------|-----------------------|
| $\rho(CH_2)$              | 912  | _          | _                     | 918,933               | ~915                  |
| $\omega(CH_2)$            | 959  | 978, 991   | 978, 995              | 964, 991              | 990                   |
| $\gamma(CH)_f$            | 972  | 1007       | 1007                  | 1009                  | _                     |
| $\gamma(CH)_{v}$          | 993  | 1019       | 1018                  | 1020                  | _                     |
| $\nu$ (C-C)               | 1158   | 1161       | 1161                  | 1159                  | 1164                  |
| $\delta(CH)_{v}$          | 1275   |            | 1284                  | 1281                  | 1281                  |
| $\delta(CH)_f$            | 1360   | 1365       | 1365                  | 1365                  | 1365                  |
| $\delta(CH_2)$            | 1420   | 1429       | 1425                  | 1425                  | 1425                  |
| $\nu(C = C)$              | 1625   | 1612       | 1616                  | 1614                  | 1618                  |
| $\nu$ (C=O)               | 1724   | 1676       | 1670                  | 1672, 1686            | 1650                  |
| $\nu$ (C=O)               | _  | 1687, 1696 | 1691                  | 1703                  | 1699                  |
| $\nu(CH)_f$               | 3069   | 2704       | n/a                   | n/a                   | 2705                  |
| $2\delta(CH)_{v}$         | _  | 2774       | n/a                   | n/a                   | 2766                  |
| $\nu_{\rm s}({\rm CH_2})$ | 2998   | 2823       | n/a                   | n/a                   | 2820                  |
| $\nu_{\rm a}({\rm CH_2})$ | 3103   | 2864       | n/a                   | n/a                   | 2857                  |

for cis-acrolein. Previous studies have shown that trans-acrolein is the most stable form, and we do not observe any features indicating cis-acrolein on Ag(111). Assignment of the peaks seen here to the vibrational modes of trans-acrolein and comparison to the peak positions previously reported for adsorbed acrolein are given in Table 1.

Fig. 2 shows the TPD spectra versus acrolein coverage on Ag(111). The peak at 164 K corresponds to desorption of the monolayer. For coverages above 1 ML, two peaks appear at 143 and 134 K, while the desorption temperature and area of monolayer peak remains the same. The 134 K peak corresponds to acrolein multilayers, while the 143 K peak is presumably due to the first layer on top of the monolayer.

Fig. 3 shows RAIR spectra after 1.56 ML of acrolein was adsorbed on Ag(111) at 85 K, annealed to various temperatures for one minute, and re-cooled to 85 K. Annealing allows more stable adsorption structures to be accessed by overcoming kinetic barriers that trap less stable structures that form upon

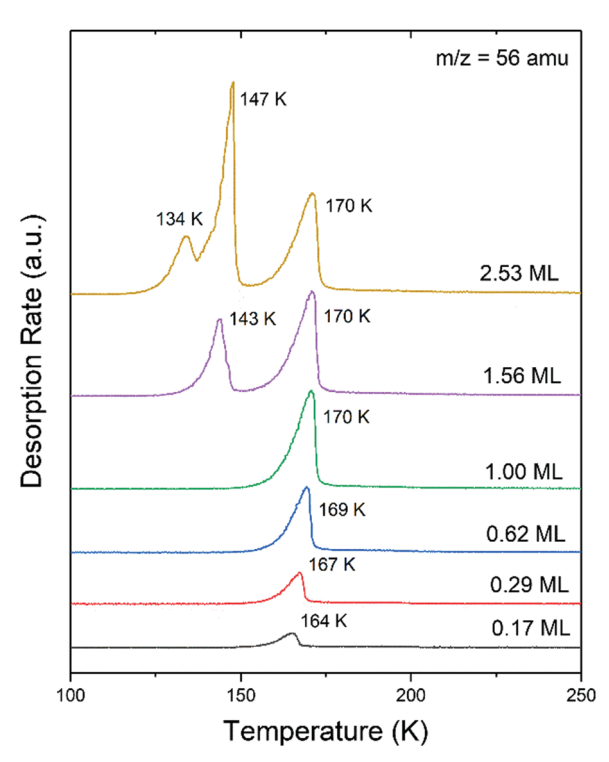


Fig. 2 TPD spectra of acrolein adsorbed on Ag(111) with increasing coverage.

adsorption at 85 K. Upon annealing to 130 K, which according to Fig. 2 should desorb the multilayer, the out-of-plane CH bends (1002 and 1022 cm<sup>-1</sup>) become less intense and the two C=O stretches at 1668 and 1685 cm<sup>-1</sup> become well separated. The 140 K anneal desorbs the second-layer molecules, which results in marked changes in the spectra. The peaks at 1022 cm<sup>-1</sup> (vinyl CH bend) and 1685 cm<sup>-1</sup> (C=O stretch) are lost, but peaks at 980, 1002, and 1673 cm<sup>-1</sup> remain with relative intensities similar to those seen in Fig. 1 at 0.17 and 0.29 ML. The way the different C=O stretch peaks respond to annealing clearly indicates that they are associated with different adsorption structures. After the 150 K anneal, there are no C=O stretch peaks but the CH<sub>2</sub> wag is still present, although broad. This spectrum is different from any seen in Fig. 1, which indicates that annealing to 150 K produces a stable monolayer, or submonolayer, structure in which all the acrolein molecules are parallel to the surface.

#### 3.2 Propanal

Fig. 4 shows RAIR spectra of propanal *versus* coverage after adsorption at 85 K. Table 2 compares the peaks observed here and their assignments with those of gas and solid phase propanal and propanal on Pd(111). At 0.07 ML, two prominent peaks at 948 and 2960 cm<sup>-1</sup> are seen, corresponding to the CH<sub>3</sub> rock and the CH<sub>2</sub> asymmetric stretch. At 0.14 ML, a peak at 1451 cm<sup>-1</sup> appears, due to the CH<sub>3</sub> asymmetric bend. There is a pronounced change in the spectra as the propanal coverage is increased from 0.14 to 0.34 ML. The 948 cm<sup>-1</sup> peak vanishes and two C=O stretch peaks are observed at 1686 and 1730 cm<sup>-1</sup>. While the peaks observed for higher coverages have similar frequencies to those of solid propanal, the 948 cm<sup>-1</sup> peak is an

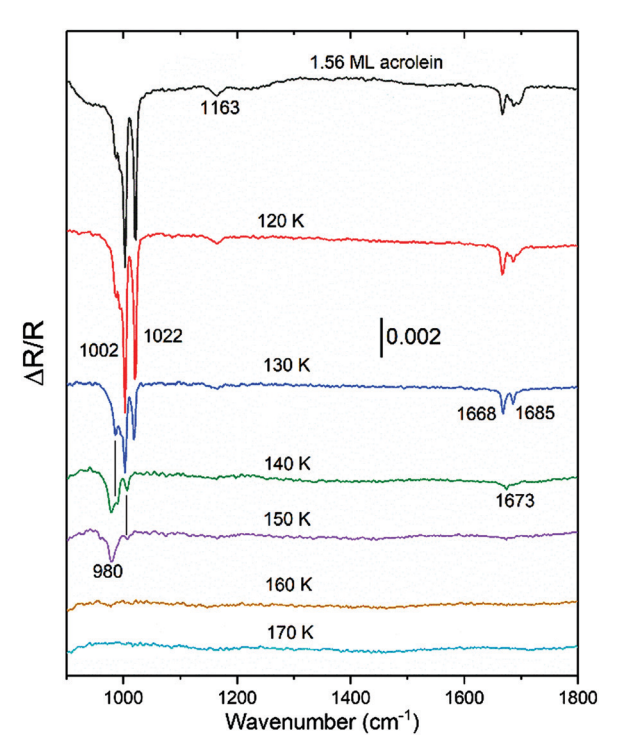


Fig. 3 RAIR spectra of 1.56 ML acrolein adsorbed on Ag(111) at  $85 \, \text{K}$  (black). The surface was annealed to the indicated temperature for one minute and re-cooled to  $85 \, \text{K}$ .

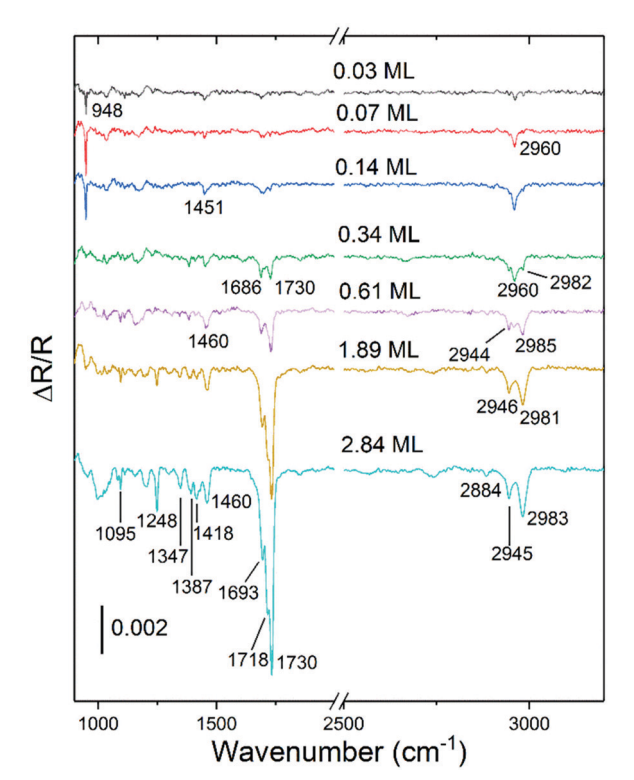


Fig. 4 RAIR spectra of propanal adsorbed on Ag(111) at  $85\ \mathrm{K}$  with increasing coverage.

exception, indicating that the CH<sub>3</sub> rock is significantly shifted through bonding of the molecule to the surface. Two closely spaced C=O stretch peaks are also observed in the liquid and

**PCCP Paper** 

Table 2 Comparison of vibrational assignments for propanal

| Vibrational mode                           | Gas <sup>14,30</sup> | Solid <sup>29</sup> | Ag(111) | Pd(111) <sup>21</sup> |
|--|----------------------|---------------------|---------|-----------------------|
| $\rho(CH_3)$                               | 892                  | 897, 902            | 948     | _                     |
| $\rho(CH_3)$                               | 1098                 | 1095                | 1095    | 1095                  |
| $\tau(CH_2)$                               | 1250                 | 1260                | 1248    | _                     |
| $\omega(CH_2)$                             | 1338                 | 1368, 1370          | 1347    | 1358                  |
| $\delta(CH)$                               | 1364                 | 1390                | 1387    | 1370                  |
| $\delta(CH_3)$                             | 1395                 | 1411, 1414          | 1418    | 1413                  |
| $\delta_{\rm a}({ m CH_2})$                | 1459                 | 1465, 1472          | 1460    | 1455                  |
| $2\rho(CH_3)$ FR $\nu(C=O)$                | 1693                 | 1695                | 1686    | 1663, 1695            |
| $\nu$ (C=O) FR 2 $\rho$ (CH <sub>3</sub> ) | 1754                 | 1730                | 1730    | 1728                  |
| $\nu$ (CH)                                 | 2812                 | 2863, 2868          | _       | 2868                  |
| $\nu_{\rm s}({\rm CH_3})$                  | 2906                 | 2877, 2879          | 2884    | 2884                  |
| $\nu_{\rm s}({\rm CH_2})$                  | 2914                 | 2939                | 2944    | 2943                  |
| $\nu_{\rm a}({\rm CH_2})$                  | 2954                 | 2966, 2968          | 2960    | 2904                  |
| $\nu_{\rm a}({ m CH_3})$                   | 2981, 2992           | 2981, 2982          | 2983    | 2960, 2987            |

polycrystalline phases of propanal and are attributed to a Fermi resonance between the C=O stretch and the first overtone of the CCC symmetric stretch<sup>14</sup> or the first overtone of the CH<sub>3</sub> rock.<sup>29</sup> The 1730 cm<sup>-1</sup> peak increases in intensity with coverage and is the most intense in the spectra for coverages of 0.61 ML and above, and is a characteristic of solid propanal. <sup>14</sup> A shoulder is observed at 1718 cm<sup>-1</sup> at 2.84 ML, which was not reported for solid propanal. Several other peaks are also visible in the 2.84 ML spectrum at 1095, 1248, 1347, 1460, and 2884 cm<sup>-1</sup>.

In the C-H stretch region, there is also an abrupt change in the spectra between 0.14 and 0.34 ML. At the three lowest coverages, a single peak is seen at 2960 cm<sup>-1</sup> but for higher coverages peaks at higher and lower wavenumbers appear that grow in intensity. At 2.84 ML the 2960 cm<sup>-1</sup> peak is no longer visible. Instead, the main peaks are at 2983 and 2945 cm<sup>-1</sup>, and a new weaker peak at 2884 cm<sup>-1</sup> becomes apparent. We assign these four C-H stretch peaks to  $\nu_s(\text{CH}_3)$  (2884 cm<sup>-1</sup>),  $\nu_s(\text{CH}_2)$  (2944-2946 cm<sup>-1</sup>),  $\nu_{as}(CH_2)$  (2960 cm<sup>-1</sup>), and  $\nu_{as}(CH_3)$  (2981–2985 cm<sup>-1</sup>). The carbonyl C-H stretch is not observed.

The TPD spectra of propanal on Ag(111) are shown in Fig. 5. A desorption peak at 159-166 K is observed for the monolayer, slightly lower than seen for acrolein in Fig. 2. Unlike for acrolein, for propanal coverages above 1 ML there is only a single multilayer desorption peak at 135 K, compared to the peak at 134 K in Fig. 2 for acrolein.

Fig. 6 shows RAIR spectra following adsorption of 0.61 ML of propanal at 85 K and annealing to the indicated temperatures. At 85 K, peaks are seen at 1450, 1689, 1725, 2958, and 2981 cm<sup>-1</sup>. The 85 K spectrum in Fig. 6 should be the same as the 0.61 ML spectrum in Fig. 4. The slight differences presumably arise from slight differences in coverage. There are only modest changes in the spectra with subsequent annealing, indicating that the structure adopted by the propanal molecules at this coverage upon adsorption at 85 K is retained up to 160 K. No peaks are observed after annealing to 170 K, which indicates complete molecular desorption, consistent with the monolayer desorption temperature of 159-166 K seen in Fig. 5.

## 3.3 2-Propenol

Fig. 7 shows RAIR spectra versus coverage for 2-propenol exposed to Ag(111) at 85 K. For submonolayer coverages, there

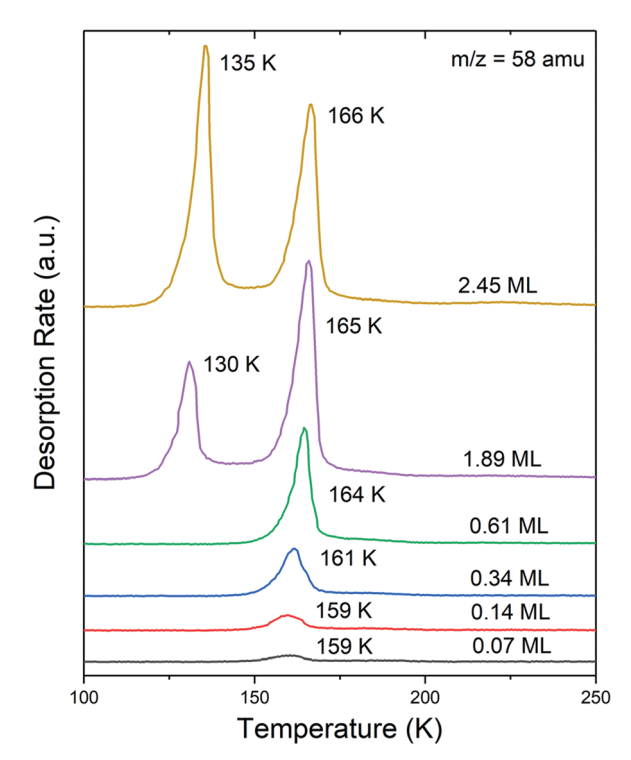


Fig. 5 TPD spectra of propanal adsorbed on Ag(111) at 85 K with increasing coverage.

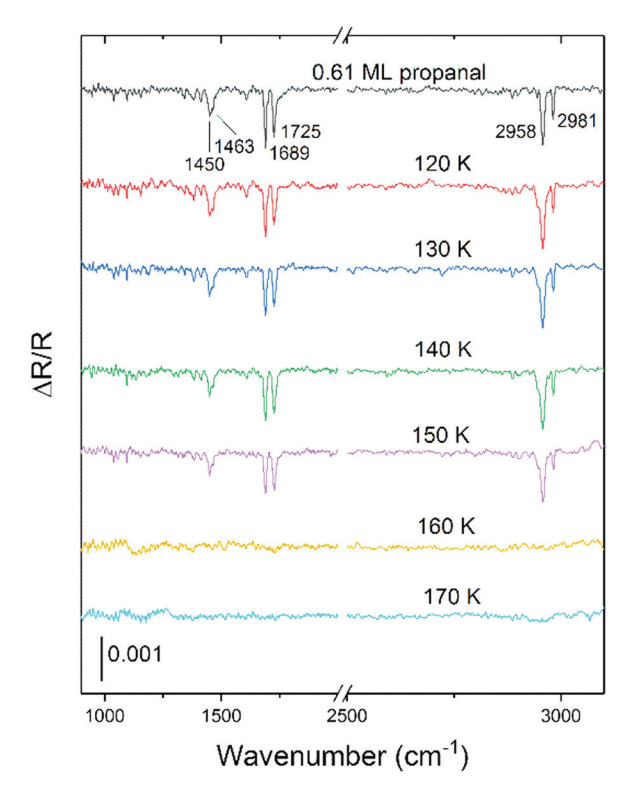


Fig. 6 RAIR spectra of 0.61 ML propanal adsorbed on Ag(111) at 85 K (black). The surface was annealed to the indicated temperature for one minute and re-cooled to 85 K.

are five distinct peaks at 925, 979, 992, 1014, and 3095 cm<sup>-1</sup>. These five peaks are assigned to the =CH<sub>2</sub> in-plane rock, the

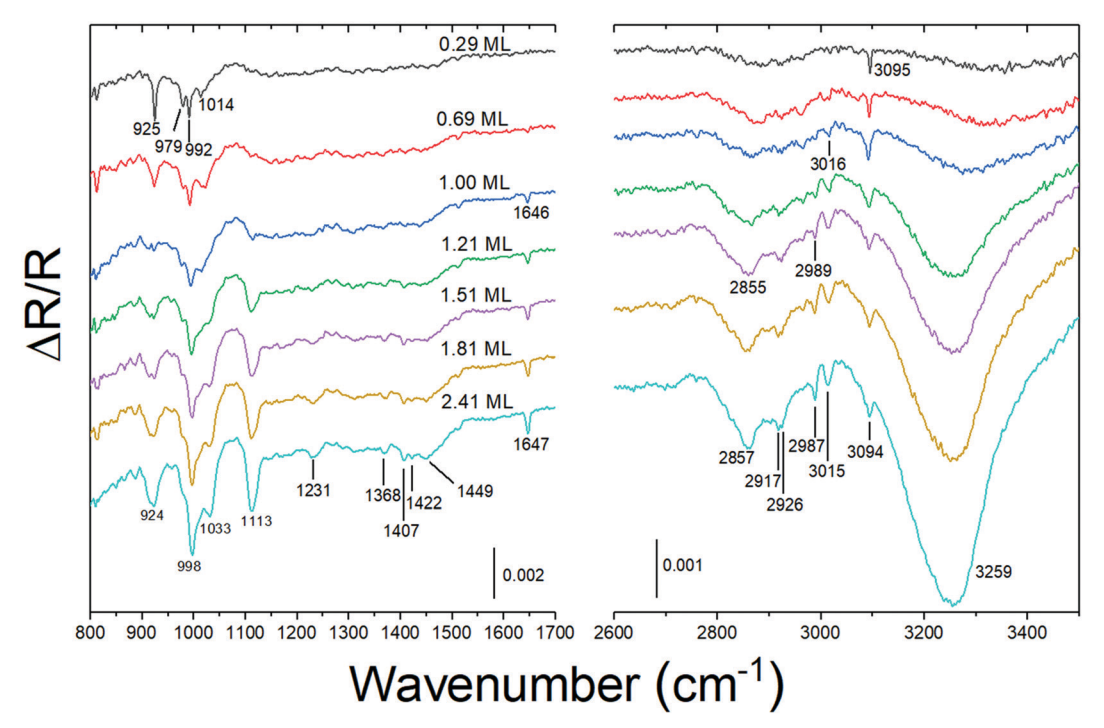


Fig. 7 RAIR spectra of 2-propenol adsorbed on Aq(111) at 85 K with increasing coverage.

 $CH_2$  rock,  $=CH_2$  wag, the CO stretch, and the  $=CH_2$  asymmetric stretch. With increasing coverage from 0.29 to 0.69 ML, the 925 cm<sup>-1</sup> peak is broadened and becomes less intense while the 992 cm<sup>-1</sup> peak increases in intensity.

Upon reaching 1 ML of 2-propenol, the IR peaks at 1113, 1646, and 3016 cm<sup>-1</sup> appear and are assigned to the C-C stretch, the C=C stretch, and the =CH<sub>2</sub> symmetric stretch. For multilayer coverages, the bending modes of the =CH<sub>2</sub>, C-H, O-H groups, and the stretching modes of the CH<sub>2</sub> and CH groups become visible. As the coverage increases past 2 ML, all these peaks grow in intensity. A complete assignment of the vibrational modes is given in Table 3. Table 3 also presents the reported frequencies for the three most stable conformers of gas phase 2-propenol. The values of the C-C and C-O stretches for 2-propenol on Ag(111) most closely match those of the Gg conformer of gas phase 2-propenol, although the broadness of the peaks may mask peaks of the other conformers. The strongly red-shifted and broad O-H stretch at 3259 cm<sup>-1</sup> for 2.41 ML is clear indication of hydrogen bonding.

The TPD spectra of 2-propenol on Ag(111) shows the monolayer desorption peak at 202 K, with the multilayer peak at 176 K (Fig. 8). Upon annealing 1.96 ML of 2-propenol, no change is seen in the RAIR spectra up to 140 K (Fig. 9). When annealing to 160 K for one minute, and re-cooling to 85 K, we observe a slight decrease in intensity for the 998, 1028, 1113, 1646, and 3251 cm<sup>-1</sup> peaks. Upon annealing to 180 K, a sharp peak at 928 cm<sup>-1</sup> appears and the 987 and 1024 cm<sup>-1</sup> peaks become distinct and sharp. This is somewhat similar to the 0.29 ML spectrum in Fig. 7 in the low wavenumber region, but whereas a broad C–H stretch is observed at 2885 cm<sup>-1</sup> in Fig. 9, a single sharp C–H stretch is seen at 3095 cm<sup>-1</sup> in Fig. 7. The

**Table 3** Comparison of vibrational assignments for 2-propenol. The gas phase values are for the different rotational conformers

| Vibrational<br>mode       | Gas phase (Gg) <sup>15</sup> | Gas phase (Cg) <sup>15</sup> | Gas phase (Ct) <sup>15</sup> | Ag(111) | Pd(111) <sup>21</sup> |
|---------------------------|------------------------------|------------------------------|------------------------------|---------|-----------------------|
| $\rho(=CH_2)$             | 938                          | _                            | _                            | 925     | _                     |
| $\tau(=CH_2)$             | 908                          | 919                          | _                            |         | ~910                  |
| $\rho(CH_2)$              | 918                          | 966                          | _                            | 979     |                       |
| $\omega(=CH_2)$           | 994                          | 1000                         | 982                          | 992     | $1000, \sim 995$      |
| ν(-C-O-)                  | 1038                         | 1103                         | 1131                         | 1033    | ~1030                 |
| ν(-C-C-)                  | 1115                         |                              | _                            | 1113    | 1113                  |
| $\tau(CH_2)$              | 1202                         | 1191                         | _                            |         |                       |
| $\delta(CH)$              | 1286                         | _                            | _                            | 1231    | 1235                  |
| $\omega(CH_2)$            | 1320                         | 1383                         | 1436                         |         |                       |
| $\delta(OH)$              | 1371                         | 1332                         | 1206                         | 1368    | 1373                  |
| $\delta(=CH_2)$           | 1427                         | 1412                         | 1390                         | 1407    | 1406                  |
|                           |                              |                              |                              | 1422    | 1424                  |
|                           |                              |                              |                              | 1449    | 1450                  |
| $\delta(CH_2)$            | 1461                         | 1472                         | _                            | _       | _                     |
| ν(C==C)                   | 1655                         | 1647                         | _                            | 1647    | 1648                  |
| $\nu_{\rm s}({ m CH_2})$  | 2875                         | 2883                         | _                            | 2857    | 2850                  |
| $\nu_{\rm a}({\rm CH_2})$ | 2933                         |                              | _                            | 2917    | 2920                  |
| $\nu_{\rm s}(=CH_2)$      | 2990                         | 3031                         | 3034                         | 2987    | 2989                  |
| $\nu$ (CH)                | 3022                         | 2999                         | _                            | 3015    | 3013                  |
| $\nu_{\rm a}(=CH_2)$      | 3093                         | 3102                         | 3118                         | 3095    | 3092                  |
| $\nu$ (OH)                | 3656                         | 3650                         | 3689                         | 3259    | 3260                  |

C—C stretch 1646 cm<sup>-1</sup> disappears upon annealing to 180 K as does the O–H stretch at 3251 cm<sup>-1</sup>. According to the TPD results in Fig. 8, annealing to 180 K should desorb any multilayer molecules, leaving only molecules bound to the surface. The loss of the C—C stretch and hydrogen-bonded O–H stretch, suggests that in the monolayer 2-propenol adsorbs with the C—C bond parallel to the surface. The sharper peaks in Fig. 9 relative to those in Fig. 7 may be due to conversion to the most stable conformer of other conformers present after adsorption

**PCCP Paper** 

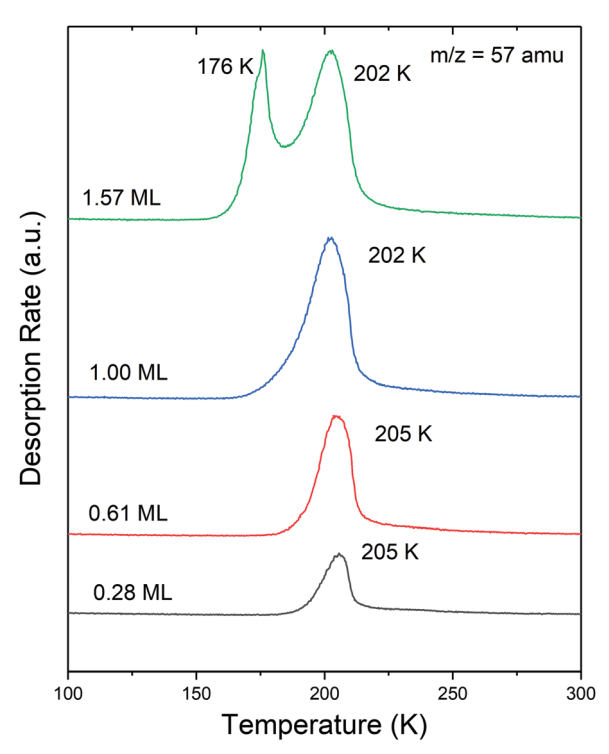


Fig. 8 TPD spectra of 2-propenol adsorbed on Ag(111) at 85 K with increasing coverage

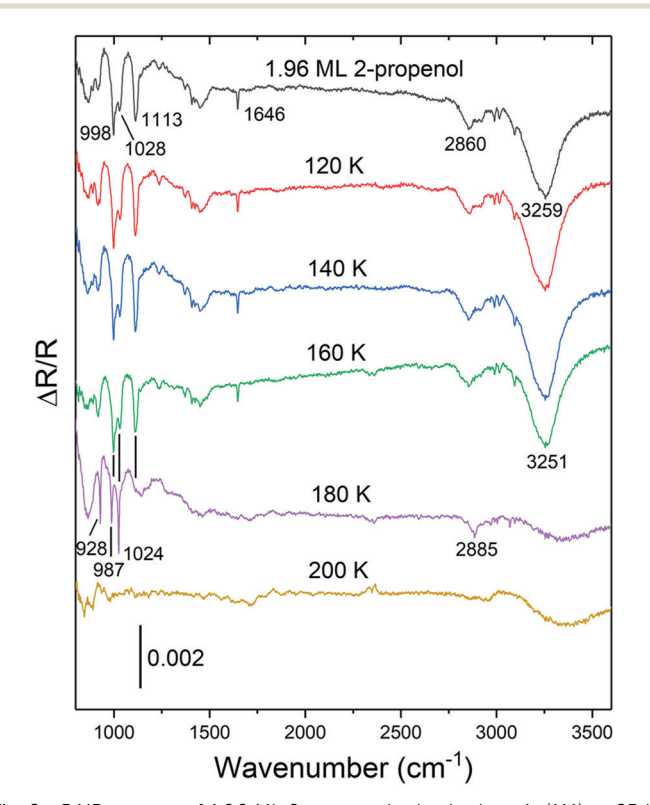


Fig. 9 RAIR spectra of 1.96 ML 2-propenol adsorbed on Ag(111) at 85 K (black). The surface was annealed to the indicated temperature for one minute and re-cooled to 85 K.

at 85 K. Annealing further to 200 K should lead to complete desorption, so that any remaining features are due to artefacts. In particular, the broad dip from 3100 to 3500 cm<sup>-1</sup> is likely due to miscancellation of a feature due to ice formation in the IR detector. The comparison between the 180 and 200 K spectra implies that there is little or no hydrogen bonding between monolayer 2-propenol molecules.

#### 3.4 1-Propanol

Fig. 10 shows RAIR spectra versus coverage for 1-propanol at 85 K. At 0.09 ML, a single peak is seen at 2953 cm<sup>-1</sup> corresponding to the CH<sub>2</sub> asymmetric stretch. At 0.23 ML, additional peaks in the CH stretch region at 2880, 2914, and 2969 cm<sup>-1</sup> appear and are assigned to the symmetric and asymmetric stretches of the CH<sub>3</sub> and CH<sub>2</sub> groups (Table 4). The CH<sub>2</sub> bend at 1456 cm<sup>-1</sup> is also first observed in the 0.23 ML spectrum. At 0.42 ML two peaks at 1015 and 1050 cm<sup>-1</sup> also appear, and are close to gas phase fundamentals at 1013 and 1066 cm<sup>-1</sup>.

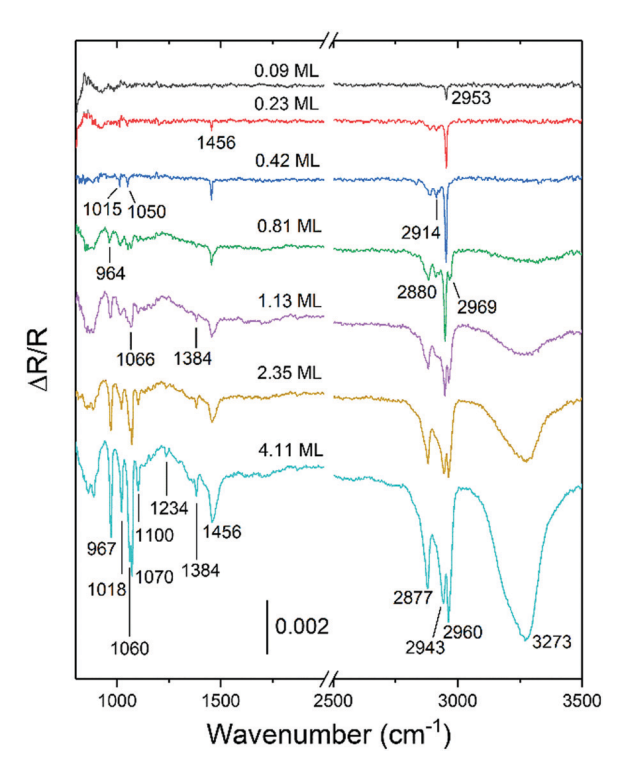


Fig. 10 RAIR spectra of 1-propanol on Ag(111) at 85 K with increasing coverage.

Table 4 Comparison of vibrational assignments for 1-propanol

| Vibrational mode           | Gas phase <sup>17</sup> | Ag(111)    | Cu(111) <sup>24</sup> | Rh(111) <sup>25</sup> |
|----------------------------|-------------------------|------------|-----------------------|-----------------------|
| $\nu_{\rm a}$ (C-C-O)      | 971                     | 967        | 972                   | 1040                  |
| $\nu_{\rm a}({\rm C-C-C})$ | 1013                    | 1018       | 1023                  |                       |
| $\rho(CH_3) + \nu(CC)$     | 1066                    | 1070, 1100 | 1103, 1074            |                       |
| $\rho(CH_2)$               |                         | _          | _                     | 1390                  |
| $\delta$ (COH)             | 1218                    | 1234       | 1239                  |                       |
| $\tau(CH_2)$               |                         | _          | 1294                  |                       |
| $\omega(CH_2)$             | 1393                    | 1384       | 1365                  |                       |
| $\delta(CH_2)$ -scissor    | 1464                    | 1456       | 1475                  | 1495                  |
| $\nu_{\rm s}({\rm CH_2})$  | 2892                    | 2877       | 2877                  | 2970                  |
| $\nu_{\rm a}({\rm CH_2})$  |                         | 2943       | 2937                  |                       |
| $\nu_{\rm a}({\rm CH_3})$  | 2978                    | 2960       | 2965                  | 2970                  |
| $\nu$ (OH)                 | 3687                    | 3273       | 3275                  | 3205                  |

Modes in this range are a mix of CCC stretch and CH<sub>3</sub> rock internal coordinates. For multilayer coverages, the 1456 cm<sup>-1</sup> peak is broadened and all the peaks observed at lower coverages increase in intensity. In addition, for coverages of 0.81 ML and above, a broad red-shifted OH stretch is observed indicating hydrogen-bonding between the 1-propanol molecules. The peaks observed here are compared to previous surface studies and to peak positions for gas phase 1-propanol in Table 4.

Fig. 11 shows the TPD spectra of 1-propanol on Ag(111). Of the four molecules, it has the highest desorption temperature for the monolayer at 219 K. It also has the highest multilayer desorption temperature, with a peak at 184 K for 4.11 ML.

Fig. 12 shows RAIR spectra after adsorbing 4.11 ML of 1-propanol on Ag(111) at 85 K and after annealing to the indicated temperatures. No changes are observed for annealing temperatures of 160 K and below. However, pronounced changes are seen for the 180 K anneal, which should desorb the multilayer. Several peaks disappear, including the OH stretch, indicating that as was the case for 2-propenol, there is no hydrogen bonding in the monolayer. The 180 K spectrum shows unusually sharp peaks at 1015, 1051, 1455, 2884, 2913, and 2948 cm<sup>-1</sup>. The 180 K spectrum in Fig. 12 is similar to the unannealed spectrum of 0.42 ML of 1-propanol (Fig. 10, blue). Further annealing to 200 K shows only the initial low coverage peak at 2948 cm<sup>-1</sup> before desorption at 220 K and loss of all IR features.

The sharpness of the peaks for the 180 K spectrum in Fig. 12 was further investigated by increasing the resolution from 4 cm<sup>-1</sup> to 1 cm<sup>-1</sup>. This gave intrinsic FWHM (full width half maxima) of 1.1, 2.1, 1.6, and 4.0 cm<sup>-1</sup> for the peaks at 1015,

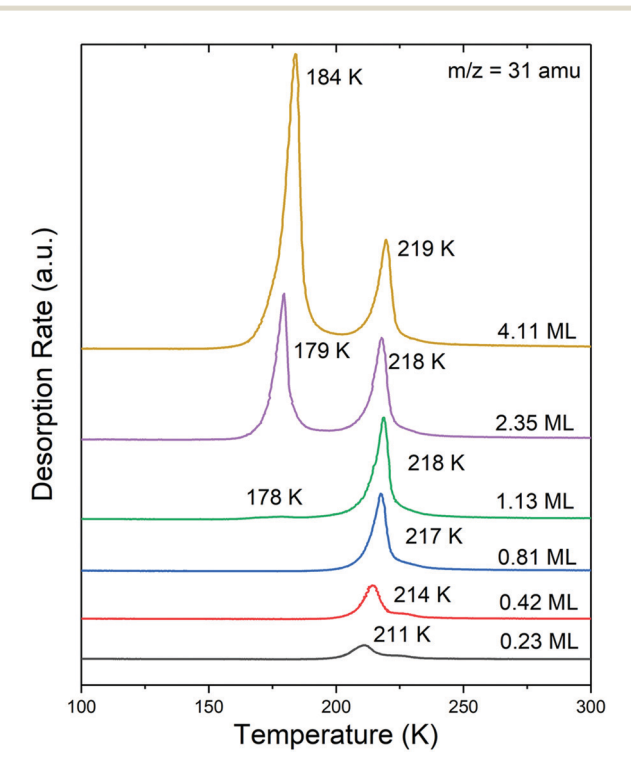


Fig. 11 TPD spectra of 1-propanol on Ag(111) adsorbed at 85 K with increasing coverage.

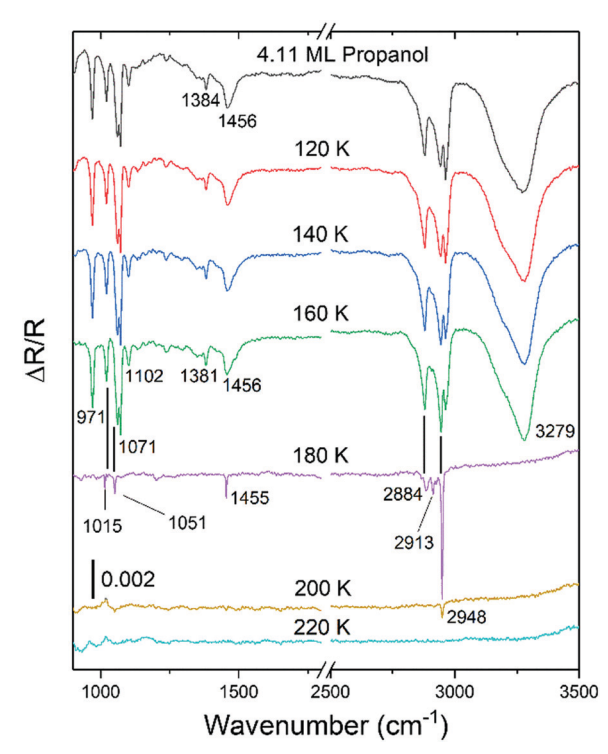


Fig. 12 RAIR spectra of 4.11 ML of 1-propanol adsorbed on Ag(111) at 85 K (black). The surface was annealed to the indicated temperature for one minute and re-cooled to 85 K

1051, 1455, and 2948 cm<sup>-1</sup>, respectively. The intrinsic FWHM were based on the assumption that the squares of the intrinsic FWHM and the instrumental resolution add to give the square of the measured FWHM. This suggests that annealing produces a well ordered monolayer with minimal inhomogeneous broadening. It also suggests that 1-propanol adsorbs as a single conformer, rather than as a mixture of conformers.

## 4. Discussion

## 4.1 RAIRS and the adsorption geometry of acrolein on Ag(111)

Selectivity in the catalytic hydrogenation of unsaturated aldehydes is often assumed to depend on the relative interaction of the C—C and C—O bonds with the surface. Brandt et~al. used NEXAFS to determine the orientation of the two bonds at acrolein coverages on Ag(111) of 0.45 and 0.85 ML. This was possible because the K edge X-ray absorption  $\pi^*$  resonances of the carbonyl carbon and the two carbon atoms of the C—C bond are easily resolved. They concluded that at the lower coverage, the C—O and C—C bonds were tilted away from the surface by  $2^\circ$  and  $6^\circ$ , respectively, whereas at 0.85 ML the tilt angle of the C—O bond remained the same, but the tilt of the C—C bond increased to  $12^\circ$ . In principle, similar information can be provided from the analysis of RAIR spectra, with a particular focus on the intensities of the C—O and C—C stretching peaks.

Previous work makes a detailed consideration of the relationship between the adsorption structure and the vibrational spectrum of acrolein on Ag(111) feasible. As a planar molecule, the 18 normal modes of acrolein can be classified as either symmetric (13A' modes)

PCCP Paper

or asymmetric (5A" modes) with respect to reflection through the molecular plane. In the context of their RAIRS study of acrolein on a Ag film, Fujii et al. performed a complete normal mode analysis of gas phase acrolein and obtained expressions for the composition of the normal coordinates in terms of appropriate symmetry coordinates.  $^{19}$  The nominal C—O stretch mode was found to consist of 75% (potential energy distribution) C=O stretch, while the C=C stretch mode consisted of 57% C=C stretch, with most of the remainder being a mix of HCH and HCC bending. Both modes are of A' symmetry for the isolated molecule. Puzzarini et al. performed several types of high-level theoretical calculations of the vibrational spectrum of gas phase acrolein (for both the trans and cis isomers) that included infrared intensities and corrections due to anharmonicity. 11 In addition to RAIR spectra of acrolein on a Ag film, Itoh and co-workers also presented transmission IR spectra of a thick ice of acrolein deposited on a KBr window at 90 K19 and RAIR spectra of acrolein on Ag(111). 18 As the molecules in frozen acrolein can be assumed to be randomly oriented, the intensity ratio of the C=O stretch to the C=C stretch of roughly 30:1 (as estimated from spectrum f in Fig. 3 of Fujii et al. 19) can be compared to the intensity ratio of 74:1 for the type of calculation that gave the best match to the experimental frequencies.<sup>11</sup>

The NEXAFS result clearly indicated that acrolein adsorbs on Ag(111) with the molecular plane approximately parallel to the surface. In terms of the vibrational modes, in such a geometry the molecular plane is no longer a symmetry plane and the modes of A' symmetry (in plane modes) for the gas phase molecule would not be forbidden by the surface selection rules. Thus, even for a strictly parallel orientation, the C=O and C=C stretch modes would still be allowed and their mere observation cannot be taken as an indication that the corresponding bonds are tilted away from the surface. From the calculations of Puzzarini et al., the intensity ratio of the most intense A' mode (the C=O stretch) to the most intense A" mode (CH<sub>2</sub> wag) is 5:1. Thus the greater intensity of the CH<sub>2</sub> wag than the C=O stretch in the RAIR spectra of acrolein at low coverage in our spectra and in the previous spectra of Itoh and coworkers 18,19 is clear evidence that the molecule is essentially parallel to the surface. Because of the marked differences in the intrinsic intensities of the C=O and C=C stretches, the observation of the C=O stretch but not the C=C stretch cannot be interpreted as indicating that the latter bond is parallel to the surface while the former is tilted away from the surface.

Although the RAIRS results cannot verify the tilt angles of the C=O and C=C bonds derived from NEXAFS, Fujii *et al.* noted that the spectra indicate that multiple forms of acrolein adsorb on Ag.<sup>19</sup> These forms were explored through DFT calculations by Ferullo *et al.*<sup>31,32</sup> They showed that while acrolein adsorbs flat on the surface at low coverages, as the coverage increases two types of superstructures form in which pairs of acrolein molecules interact in either a head-to-tail fashion with the molecular planes parallel to the surface, or in a head-to-head structure with some molecules highly tilted on the surface. The multiple forms of acrolein indicated by the RAIRS results could be associated with the different superstructures, or to molecules that are and are not part of the superstructures. The C=O tilt angle

derived from fitting the NEXAFS data would then represent a weighted average among the various forms of adsorbed acrolein.

#### 4.2 Propanal, 2-propenol, and 1-propanol

Although the four molecules share a CCCO skeleton, the different number of H atoms gives rise to different possibilities for bonding to the Ag(111) surface. The TPD results show that the molecules with the highest monolayer desorption temperatures also have the highest multilayer desorption temperatures. This indicates that the factors that lead to stronger intermolecular interactions also lead to a stronger interaction with the surface. The clear separation between multilayer and monolayer desorption temperatures permitted RAIR spectra to be obtained after desorbing the multilayer, so that the spectra obtained were characteristic of the molecules bonding to the surface. In the case of the two alcohols, the multilayer RAIR spectra revealed strong hydrogen bonding between the molecules, which was not present for the monolayers. The addition of hydrogen bonding to the intermolecular binding would account for the higher multilayer desorption temperatures of the two alcohols. As 1-propanol had the highest monolayer desorption temperature, this suggests that bonding to the surface via an O atom lone pair of an OH group produces the strongest bonding. Like acrolein, 2-propenol has a C=C double bond and its C=C stretch is clearly observed for the multilayer, but when the multilayer is desorbed this peak disappears along with the O-H stretch. The simple explanation is that the C=C bond is parallel to the surface for the monolayer. This might imply  $\pi$ -bonding to the surface, but this doesn't lead to stronger bonding than for 1-propanol, where no  $\pi$ -bonding is possible. The most weakly held molecule is propanal, which has neither an OH bond nor a C=C bond. The RAIR spectra for propanal versus coverage show an abrupt change between 0.14 and 0.34 ML, implying that the molecule adopts very different structures at high and low submonolayer coverages. The simplest explanation is that at the lowest coverage, the molecule bonds with the CCHO plane parallel to the surface, but as the molecules become more crowded, they adopt a more upright orientation with the C=O bond no longer parallel to the surface. In the parallel orientation, the molecule could bind to the surface via a  $\pi$  bond of the C=O group  $(\eta^2-\pi(CO))$ . This is evidently quite weak, as it is easily disrupted by crowding. The annealing experiments with propanal show little change with annealing temperature, indicating that the structure adopted at higher coverages is stable.

#### 4.3 Implications for acrolein hydrogenation

The results presented here have implications for acrolein hydrogenation on Ag(111). The RAIR spectra clearly indicate that acrolein adsorbs in more than one form, and that the relative number of the different forms depend on coverage. It is possible that the selectivity dependence on acrolein coverage is associated with a difference in reactivity of the differently oriented molecules in the different superstructures. The adsorption properties of 2-propenol and propanal may also influence the selectivity in the partial hydrogenation of acrolein. Once hydrogenation forms 2-propenol, its higher desorption temperature than that of propanal means it would be more likely

to undergo additional hydrogenation to 1-propanol. The conclusion that in their stable monolayer adsorption geometries, the C—C bond of 2-propenol is parallel to the surface whereas the C—O bond of propanal is not, also implies that the former is more likely than the latter to undergo complete hydrogenation.

Acrolein hydrogenation on Ag(111) likely takes place through formation of a stable surface intermediate, formed by adding a single H atom. The addition of a second H atom to this intermediate would then determine the relative selectivity to 2-propenol or propanal. This is suggested by the results of Brandt *et al.* where upon acrolein hydrogenation both propanal and 2-propenol desorb by reaction-limited kinetics at higher temperatures than those they desorb at when they are each exposed to the Ag(111) surface independently. Dosert *et al.* used RAIRS to study acrolein hydrogenation over a Pd(111) surface and identified the intermediate to 2-propenol formation as propenoxy,  $H_2C$ — $CHCH_2O$ —, with the C—C bond oriented perpendicular to the surface and bonding to the surface *via* a single  $\sigma$  bond between the O atom and a Pd atom. We are currently seeking to identify any intermediates that might form in the hydrogenation of acrolein on Ag(111).

## 5. Conclusion

Using a combination of RAIRS and TPD we have shown that each of the four related molecules, acrolein, propanal, 2-propenol, and 1-propanol, display different coverage dependent adsorption structures on Ag(111). The structures are related to the way the different functional groups of the molecules interact with the surface metal atoms. Although each molecule can exist in the gas phase as several conformers of similar energy, the spectra of the adsorbed molecules at monolayer coverages formed by annealing to desorb multilayers are consistent with a single conformer. The RAIR spectra show that 2-propenol and 1-propanol form strong intermolecular hydrogen bonds in the multilayer, consistent with the higher multilayer desorption temperatures relative to those of the other two molecules. Although the presence of C=C and C=O bonds allows for  $\pi$ -bonding to the surface, these bonds are weak relative to intermolecular interactions and bonding via an OH group.

### Conflicts of interest

There are no conflicts to declare.

## Acknowledgements

This work was supported by a grant from the National Science Foundation, CHE-1800236.

### References

- 1 P. Claus, Top. Catal., 1998, 5, 51-62.
- 2 E. A. P. Silva, J. S. Carvalho, A. G. Guimarães, R. D. S. S. Barreto, M. R. V. Santos, A. S. Barreto and L. J. Quintans-Júnior, *Expert Opin. Ther. Pat.*, 2019, 29, 43–53.

3 W. Schwab, R. Davidovich-Rikanati and E. Lewinsohn, *Plant I.*, 2008, 54, 712–732.

- 4 K. A. D. Swift, Top. Catal., 2004, 27, 143-155.
- 5 F. Delbecq and P. Sautet, J. Catal., 1995, 152, 217-236.
- 6 F. Delbecq and P. Sautet, J. Catal., 2002, 211, 398-406.
- 7 T. B. L. W. Marinelli, S. Nabuurs and V. Ponec, *J. Catal.*, 1995, **151**, 431–438.
- 8 S. Tuokko, P. M. Pihko and K. Honkala, *Angew. Chem., Int. Ed.*, 2016, 55, 1670–1674.
- K. Brandt, M. E. Chiu, D. J. Watson, M. S. Tikhov and R. M. Lambert, J. Am. Chem. Soc., 2009, 131, 17286–17290.
- 10 J. Fan and M. Trenary, Langmuir, 1994, 10, 3649-3657.
- 11 C. Puzzarini, E. Penocchio, M. Biczysko and V. Barone, J. Phys. Chem. A, 2014, 118, 6648–6656.
- 12 J. Randell, J. A. Hardy and A. P. Cox, *J. Chem. Soc., Faraday Trans.* 2, 1988, **84**, 1199–1212.
- 13 H. M. Pickett and D. G. Scroggin, J. Chem. Phys., 1974, 61, 3954–3958.
- 14 G. A. Guirgis, B. R. Drew, T. K. Gounev and J. R. Durig, *Spectrochim. Acta, Part A*, 1998, **54**, 123–143.
- 15 J. R. Durig, A. Ganguly, A. M. E. Defrawy, C. Zheng, H. M. Badawi, W. A. Herrebout, B. J. V. D. Veken, G. A. Guirgis and T. K. Gounev, J. Mol. Struct., 2009, 922, 114–126.
- 16 D. R. Truax and H. Wieser, Chem. Soc. Rev., 1976, 5, 411-429.
- 17 K. Fukushima and B. J. Zwolinski, *J. Mol. Spectrosc.*, 1968, 26, 368–383.
- 18 M. Akita, N. Osaka and K. Itoh, Surf. Sci., 1998, 405, 172–181.
- 19 S. Fujii, N. Osaka, M. Akita and K. Itoh, J. Phys. Chem., 1995, 99, 6994–7001.
- 20 L. E. Murillo and J. G. Chen, Surf. Sci., 2008, 602, 919-931.
- 21 K.-H. Dostert, C. P. O'Brien, F. Mirabella, F. Ivars-Barcelo and S. Schauermann, *Phys. Chem. Chem. Phys.*, 2016, **18**, 13960–13973.
- 22 D. A. Esan, Y. Ren, X. Feng and M. Trenary, *J. Phys. Chem. C*, 2017, **121**, 4384–4392.
- 23 D. A. Esan and M. Trenary, *Phys. Chem. Chem. Phys.*, 2017, 19, 10870–10877.
- 24 S. C. Street and A. J. Gellman, Surf. Sci., 1997, 372, 223-238.
- 25 N. F. Brown and M. A. Barteau, Langmuir, 1992, 8, 862-869.
- 26 M. Myint, Y. Yan and J. G. Chen, *J. Phys. Chem. C*, 2014, **118**, 11340–11349.
- 27 J. Gong, T. Yan and C. B. Mullins, *Chem. Commun.*, 2009, 761–763.
- 28 M. Muir and M. Trenary, J. Phys. Chem. C, 2020, 124, 14722–14729.
- 29 G. Sbrana and V. Schettino, J. Mol. Spectrosc., 1970, 33, 100–108.
- 30 B. Köroğlu, Z. Loparo, J. Nath, R. E. Peale and S. S. Vasu, J. Quant. Spectrosc. Radiat. Transfer, 2015, 152, 107–113.
- 31 R. Ferullo, M. M. Branda and F. Illas, *J. Phys. Chem. Lett.*, 2010, 1, 2546–2549.
- 32 R. M. Ferullo, M. M. Branda and F. Illas, *Surf. Sci.*, 2013, **617**, 175–182.
- 33 K.-H. Dostert, C. P. O'Brien, F. Ivars-Barceló, S. Schauermann and H.-J. Freund, *J. Am. Chem. Soc.*, 2015, **137**, 13496–13502.